Manuscript Details

Manuscript number	CCC_2019_511_
Title	OLIVE BIOMASS ASH AS AN ALTERNATIVE ACTIVATOR IN GEOPOLYMER FORMATION: A STUDY OF STRENGTH, RADIOLOGY AND LEACHING BEHAVIOUR
Article type	Research Paper

Abstract

Chemical, physical, mineralogical and radiological characterization of olive biomass fly ash (OBFA) and bottom ash (OBBA) was main objective to determine their potential use as alkaline activators in the preparation of alkali-activated materials or geopolymers. Water solubility tests showed that they released K and Na ions, affording a high pH and alkaline content. Pastes made with 70 wt.% vitreous blast furnace slag (SL) and 30 wt.% of OBFA or OBBA yielded alkali-activated materials with 28 days mechanical strength of 33 to 18 MPa. In pastes prepared with 30 wt% OBFA, strength values were comparable to those developed by slag pastes activated with a commercial KOH. However, the pastes made with 70 wt.% coal fly ash and 30 wt.% OBFA or OBBA proved to be inviable because the pH reached was not high enough to activate the precursor. The radiological calculations of OBFA- and OBBA-SL bearing pastes would conform to European legislation on protection against exposure to ionising radiation, for the activity concentration index (ACI) found in the final product was less than 1 in all cases. The pastes leached primarily K. The presence of elements such as 210Po and 210Pb at the end of the decay chain in the eluates would not limit the use of biomass ash and slag blends. These findings have confirmed the feasibility of using olive oil biomass ashes as an alternative alkaline activator in blast furnace slag systems to produce alkali-activated materials or geopolymers, with properties that make them apt for use as building materials.

Keywords	Olive biomass ash; Geopolymers; Alternative alkaline activators, Mechanical behaviour, Leaching, Natural Radioactivity

Corresponding Author	Francisca Puertas
Corresponding Author's Institution	Eduardo Torroja Institutue
Order of Authors	Francisca Puertas, Maria del Mar Alonso, Catalina Gasco Leonarte, JOSE ANTONIO SUAREZ-NAVARRO, María Martín-Morales, Montserrat Zamorano

.

OLIVE BIOMASS ASH AS AN ALTERNATIVE ACTIVATOR IN GEOPOLYMER FORMATION: A STUDY OF STRENGTH, DURABILITY, RADIOLOGY AND LEACHING

M.M. Alonso[1], C. Gascó[2*], M. Martín Morales[3], J.A. Suarez[2], M. Zamorano[3], F. Puertas[1]

1. Eduardo Torroja Institute for Construction Science (IETcc-CSIC), Madrid, Spain

2. CIEMAT, Madrid, Spain

3. University of Granada, Granada, Spain

*Corresponding author: Prof Dr Francisca Puertas. email: puertasf@ietcc.csic.es

Abstract

Chemical, physical, mineralogical and radiological characterization of olive biomass fly ash (OBFA) and bottom ash (OBBA) was main objective to determine their potential use as alkaline activators in the preparation of alkali-activated materials or geopolymers. Water solubility tests showed that they released K and Na ions, affording a high pH and alkaline content.

Pastes made with 70 wt.% vitreous blast furnace slag (SL) and 30 wt.% of OBFA or OBBA yielded alkali-activated materials with 28 days mechanical strength of 33 to 18 MPa. In pastes prepared with 30 wt% OBFA, strength values were comparable to those developed by slag pastes activated with a commercial KOH. However, the pastes made with 70 wt.% coal fly ash and 30 wt.% OBFA or OBBA proved to be inviable because the pH reached was not high enough to activate the precursor.

The radiological calculations of OBFA- and OBBA-SL bearing pastes would conform to European legislation on protection against exposure to ionising radiation, for the activity concentration index (ACI) found in the final product was less than 1 in all cases. The pastes leached primarily K. The presence of elements such as ^{210}Po and ^{210}Pb at the end of the decay chain in the eluates would not limit the use of biomass ash and slag blends.

These findings have confirmed the feasibility of using olive oil biomass ashes as an alternative alkaline activator in blast furnace slag systems to produce alkali-activated materials or geopolymers, with properties that make them apt for use as building materials.

Keywords: Olive biomass ash; Geopolymers; Alternative alkaline activators, Mechanical behaviour, Leaching, Natural Radioactivity

1. INTRODUCTION

Most countries' economic and social models have undergone profound change since the mid-twentieth century, with both a significant improvement in quality of life and a concomitant rise in energy consumption [1]. Combustion is often the primary source of energy generation in the form of heat or electricity. In Spain, the traditional use of non-renewable fuels such as coal, oil and natural gas has led to a dependence on imports for 75 % of its energy [2]. Fossil fuel combustion, has given rise to severe environmental problems, including an increase in mean global temperatures, acid rain, the greenhouse effect, and holes in the ozone layer as well as to health hazards [3] [4]. In consequence actions for sustainable development should be geared to enhancing energy production; in this regard, renewable energy resources appear to be one of the most efficient and effective solutions because they are both renewable and sustainable [5] In this sense, biomass is a desirable and sustainable alternative to traditional, non-renewable fossil fuels. According to some estimates, by 2050 from 33 % to 50 % of world energy consumption could be met by (essentially) burning biomass [6].

Combustion of biomass has the disadvantage that it generates large amounts of ashes that affect to the conversion process reducing the efficiency of the combustion systems, cause extra cost for boilers cleaning and maintenance, and hinder further utilization of biomass materials as combustion fuels [7] [8] [9]. Ash formed during biomass combustion can be divided into fly ash (BFA) and bottom ash (BBA). BFA results from the combustion of biomass and can be captured with cyclone or fabric filters or electrostatic precipitators in combustion plants; BBA forms part of the solid waste collected from the bottom of boilers. The physical, chemical and mineralogical characteristics of biomass ash and its environmental hazards depends on the nature of the biomass and the combustion technology used [10], and system used to collect the ash all play a part [11] [6] [12]. Both BFA and BBA are generally deemed to have higher Mg, K, Ca, Mn, Mo, S, Cl and P contents and greater loss on ignition than coal fly ash (CFA). In contrast, the percentage of Si, Al, Na, Fe and Ti is higher in the latter than in the former [13].

The routine practice of stockpiling biomass ash in waste pits constitutes an obvious environmental hazard, for it rules out the use of land for other purposes and may potentially contain toxic elements that could leach into and pollute the soil [14] [15] [16]. Such environmental issues, together with the growing production of this type of ash [17] [18] [19], define a need to explore sustainable applications for the waste.

Biomass ashes are presently used primarily to fertilise or recover soil, given that it is a source of plant nutrients (such as C, Ca, S, Mg, Na and P) that create a growth-favouring alkaline medium [20] [21] [22], These biomass ashes can also provide toxic or harmful elements to the soil, which would be absorbed by crops fertilised with them depending on: their specific metabolism and their facility of leaching from fertilized soil. Nonetheless, use as fertiliser does not deplete biomass ash output, estimated to come to around 500 million tonnes yearly worldwide [6] [23]. Although that is 35 % less than coal ash production (780 million tonnes/year), biomass output is growing rapidly, whereas the generation of coal ash is expected to decline significantly in the years to come. Biomass ash has also been suggested as a possible adsorbent in fired clay material manufacture [24] [25] [20]. Such biomass growing production along with environmental issues, define a need to explore sustainable applications according to circular economy strategy [17] [10] [19].

Construction material manufacture is a field where BFA and BBA use is rising and has significant growth potential. Many types of BFA and BBA (such as rice husk [26], bamboo [27] and bagasse ash [28]) exhibit substantial pozzolanicity, favouring their use as cement replacements in mortars and cements or to substitute for conventional coal ash in such applications [29]. Many studies have also shown that both BFA and BBA can be used to manufacture mortars and concretes, as replacements not only for the binder but also for the aggregate [30] [31] [32].

Ash use is not confined to conventional cements and concretes, however, for a few studies has identified the material as a potential precursor in the preparation of alkali-activated cements or geopolymers [33] [34] [35] [36]. However, to date only two papers have been published on the potential of such waste as an alkaline activator, even though biomass ash may contain high proportions of soluble alkaline compounds [37]. Peys et al. [38] explored the possibility of alkali-activating metakaolin with high-potassium corn ash. Font et al. [39], in turn, used olive-stone biomass ash to prepare alkali-activated slag mortars.

Olive oil is a product of particular importance within the Mediterranean and Spanish agricultural food system, owing to be the world's largest producer area. The residues from olive oil industries could be used as biomass for energy production in combustion plants, and two types of ash are produced: biomass fly ash (BFA) and biomass bottom ash (BBA) The potential of precisely this type of biomass waste, generated by the olive oil industry, has not been studied in depth. Spain, and more specifically its southern region, Andalusia, is the world leader in olive oil output, with nearly 1.4 million hectares of olive crops generating over 4.2 million tonnes/year of pruning, olive stone and similar waste [40] [29] [4]. As olive biomass ash exhibits no pozzolanic activity due to its low $SiO_2 + Al_2O_3$ content (<70 wt. %), it cannot be used as an active addition in portland cement [29] [41] [42]. In fact, replacing 10 wt. % of binder with olive biomass fly ash (OBFA) has been shown to reduce mechanical strength by over 30 % [42]. Recently, olive biomass fly ash (OBFA) and olive biomass bottom ash (OBBA) have been used as pore-forming agents in ceramic materials [43] [44] [45] and as a replacement for natural sand in mortars [46], limestone filler in self-consolidating concretes [47] or cement in mortars after OBBA recombustion to improve its properties [48].

As noted earlier, both OBFA and OBBA have enormous potential as possible alkaline activators in the preparation of alkali-activated cements or geopolymers. Font et al. [39] paved the way, although many unknowns have yet to be explored. Sight should not be lost of the fact that as biomass ash is deemed to be a NORM (naturally occurring radioactive material) [49] [50], its use is subject not only to mechanical, rheological and durability-related considerations, but also to the legal constraints around its use laid down in European Directive 2013/59 [51].

Moreover, in the final stage of the life of a construction material (refuse discharged into the environment), the leaching of naturally radioactive elements present in a material is of greater significance, radiologically speaking, than the gamma dose rate (ACI or activity concentration index applied in housing) they may induce where they are stockpiled. The importance of the absence of secular equilibrium in natural radioactive chains in debris lies in that the radioactive elements they contain, such as ^{210}Pb and ^{210}Po (progenitor and descendant, respectively), have not been deemed environmentally harmful. Such isotopes, ^{210}Po and ^{210}Pb, may be present in nature at activity concentrations up to 10-fold greater than the radioisotope that is head of the natural radioactive series to which belong and could be more bio-cumulative in life forms than other radionuclides in their radioactive series. Radioisotopes as ^{210}Po and ^{210}Pb may have higher activity concentrations than other isotopes from its series in biological ashes as consequence essentially of : ignition temperatures in the industrial combustion furnace and the type of fly ash obtained and the type of furnace [1]. This study explores the disequilibrium in these elements in the raw material and assesses the possible environmental implications associated with element leaching from the end cementitious materials at both the initial and final stages of their life cycle. Leaching studies are therefore essential to definitively validate the use of biomass ash as an active component in alkali-activated and geopolymer cements and concretes.

Further to the above, the working hypothesis explored here is that olive oil industry biomass ash may potentially be usable as an alkali activator for alkali-activating cementitious materials or geopolymers apt for construction and radiologically compliant and that the possible post-use release of any toxic or deleterious constituent elements into the environment can be prevented.

The study therefore pursued the following objectives:

1) To characterise the chemistry, mineralogy and radiology (inasmuch as they are NORMs) of precursors (slag and coal fly ash) and olive biomass fly and bottom ash generated by the combustion of olive industry waste in steam power plants.
2) To assess the potential of OBFA and OBBA as alternative alkaline activators to produce geopolymers, using vitreous blast furnace slag and coal fly ash as precursors, in terms of the mechanical behaviour of the blends prepared with this biomass ash.
3) To conduct radiological and leaching studies to determine the interaction of the new OBFA- and OBBA-bearing geopolymer materials with the environment.

2. EXPERIMENTAL

2.1. Materials: Chemical, mineralogical, physical and radiological characterization.

The solids used as geopolymers precursors were a vitreous blast furnace slag (SL) and coal combustion fly ash (CFA). The biomass ash used consisted in olive biomass fly ash (OBFA) and olive biomass bottom ash (OBBA) generated during the combustion of olive oil industry waste, i.e., pruning debris, leaves and first and second press olive dregs. The OBBA and OBFA samples were a proportional and homogeneous blend of the bottom and fly ash collected from three combined heat and power plants, each using a different combustion technology and all forming part of the El Tejar industrial energy complex at Palenciana in the Spanish province of Córdoba.

The chemical characterisation of all the materials was determined on a Philips PW-1004 XRF spectrometer. Loss on ignition [52], insoluble residue [53] and reactive silica values for CFA, OBFA and OBBA [54] were also determined. The vitreous content in SL was determined with the Hooton and Emery-modified McMaster method [55], while the glass content in CFA was assessed according to Arjuman et al methodology [56]. Mineralogical characterisation of both types of biomass ash was determined with XRD on a Bruker AXS D8 Advance X-ray diffractometer.

The particle size distribution of the materials used in this study was found with a Malvern Mastersizer S analyser. The particle size determined for OBFA and OBBA was not that of the initial ash; rather, after drying at 100 °C for 24 h, the samples were ground to a size of under 45 μm to obtain a high specific surface and thus optimise alkaline activation. Precursor SL and CFA were also analysed to determine their Blaine specific surface [57].

Precursors SL and CFA as well as OBFA and OBBA were also characterised radiologically via gamma spectrometry. Naturally radioactive elements ^{210}Po and ^{210}Pb were likewise analysed, using alpha spectrometry (polonium-210 directly and lead-210 indirectly, through polonium ingrowth). The Spanish CIEMAT (Energy, Environment and Technology Research Centre) Environmental Radioactivity and Radiological Surveillance Department's γ-spectrometry laboratory is equipped with 10 (two standard, two broad energy, three extended range and three reverse electrode) Canberra high purity coaxial germanium detectors with relative efficiencies ranging from 25.0 % to 115.7 % The detectors, which are located in the basement of a 50-year-old building, are protected either by 150 mm iron shielding or iron shielding lined with copper or tin to absorb the fluorescent X-rays emitted by the lead. The mean laboratory radon concentration is around 35 Bq·m^3. Radionuclides in the decay chains headed by ^{238}U, ^{232}Th and ^{40}K were determined in the samples. ^{234}Th (63 keV), ^{214}Pb (351 keV), ^{214}Bi (609, 1120 and 1765 keV) were determined in the ^{238}U series, and ^{228}Ac (911 and 969 keV), ^{212}Pb (238 keV) and ^{208}Tl (583 keV) in the ^{232}Th series. As ^{40}K (1460 keV) forms part of no series, its activity was quantified separately. This methodology was applied by the authors in an earlier study [58]. European Directive 2013/59 [38] stipulates that before building materials identified 'as being of concern' are brought to market, the activity concentration index (*I*) (Equation 1) of their radionuclides must be determined and lie below the reference level of 1 mSv·year^{-1}. Where such materials are 'liable to give doses exceeding the reference level', Member States may include specific requirements in building codes or restrictions on their envisaged use.

The activity concentration index, I, was calculated with Equation 1:

$$I = \frac{C_{226_{Ra}}}{300} + \frac{C_{228_{Ac}}}{200} + \frac{C_{40_K}}{3000} (Eq.1)$$

where: C_{226Ra} is the activity concentration of ^{226}Ra determined from ^{214}Pb; C_{232Th} is the activity concentration of ^{232}Th determined from its daughter ^{214}Pb; and C_{40K} is ^{40}K activity concentration.

Equation (2) was used to estimate the associated uncertainty (u(I)).

$$u(I) = \sqrt{\left(\frac{1}{300}\right)^2 u^2(C_{226_{Ra}}) + \left(\frac{1}{200}\right)^2 u^2(C_{228_{Ac}}) + \left(\frac{1}{3000}\right)^2 u^2(C_{40_K})} (Eq.2)$$

where; $u(C_{226Ra})$ is the activity concentration uncertainty for ^{226}Ra determined from the activity of its daughter ^{214}Pb; $u(C_{232Th})$ is the activity concentration uncertainty for ^{232}Th as determined from its radioactive daughter ^{212}Pb; and $u(C_{40K})$ is the activity concentration uncertainty for ^{40}K. ^{212}Pb was selected instead of ^{228}Ac since ^{228}Ac suffers summing-in and summing-out coincidences.

The ^{210}Po and ^{210}Pb, both of which form part of the uranium natural decay chain are key elements in the analysis

of the radioactive disequilibrium extant in their series, particularly in the case of ash from biological samples. These elements were extracted from 0.5 g of the sample by means of a wet acid digestion with ($HF/HCl/HNO_3$). The sample was maintained at a temperature<90 °C until it dissolved completely. The ^{208}Po tracer was added to the dissolved sample to determine the chemical yield. Both isotopes ^{210}Po and ^{208}Po were deposited spontaneously on silver disks using Flynn method [59], and subsequently analyzed by alpha spectrometry. The ^{210}Pb was quantified in the supernatant, waiting 3 months after spontaneous deposition of the polonium for the new ^{210}Po ingrowth. The 208Po tracer was subsequently added to determine this ^{210}Po ingrowth from 210Pb with alpha spectrometry and quantified by means of Bateman equations [60] to indirectly calculate the concentration activity of ^{210}Pb.

2.2. Viability of the use of OBFA and OBBA as potential geopolymer alkaline activators.

According to OBFA and OBBA characterization findings, a more in depth study was carried out in order to assess the viability of using both biomass ashes as alkaline activators. To that end, their water solubility ware explored and geoplymer pastes were prepared using these biomass ashes and SL and CFA as precursors.

2.2.1. OBFA and OBBA water solubility

OBFA and OBBA water solubility was determined by stirring 1 g samples in 10 g of deionised water for 2 h at 25 °C, 45 °C or 85 °C. The liquid was subsequently ultra-centrifuged and its pH determined on a Crison GLP pH-meter, while its elemental composition was determined on a Perkin Elmer Optima 8300 dual vision inductively coupled plasma optical emission spectrometer (ICP-OES).

2.2.2. Alkali-activated slag and coal fly ash pastes prepared with OBFA- and OBBA-as alkaline activators. Mechanical strengths and reactivity of the pastes

Activated blast furnace slag (SL) and coal fly ash (CFA) paste specimens (1x1x6 cm) were prepared from blends containing 70 wt. % binder or precursor (SL or CFA) and 30 wt. % biomass ash (OBFA or OBBA) and water as the sole mixing liquid, as described in Table 1.

SL or CFA/olive biomass ashes ratio (70/30), used in the preparation of the pastes, are consequence of previous tests carried out in the laboratory and on the consideration of two main aspects:

a) to ensure a sufficient content of Si, Al and/or Ca ions from precursors (CFA or SL) for the formation of an activated alkaline material. An also, to have a sufficient amount of biomass ashes, which guarantee from their partial solubilisation, an enough concentration of Na and K ions suitable for a high alkalinity and an adequate pH in the medium (as will be described and demonstrated in further sections).

b) to minimize the activity concentration index (ACI) in pastes, which would be very high, due to the use of a high percentage of olive biomass ashes. The pastes obtained would have a content of natural radioactivity admissible by European legislation for construction materials.

The l/s ratios used in the mixes (Table 1) were varied as necessary to ensure that plasticity and consistency were the same in all the pastes, whether made from SL or CFA. Each paste was cured under two sets of temperature conditions: 45 °C for 24 h and 85 °C for 24 h (both with 99 % RH). After the first 24 h all the specimens were removed from the moulds and stored in a humidity chamber at 21±2 ºC and 99 % RH for 2, 7 and 28 days.

Additionally mixes containing 100 % SL and water (SL-W) were likewise moulded into 1x1x6 cm specimens and cured at 45 °C and 85 °C, in equal conditions previous described. For the intents and purposes of comparison to a conventional activator, pastes were also prepared with SL and 2.5 M KOH (pH=13.88) at an l/s ratio of 0.45 (SL-K pastes). These pastes were maintained under the same curing conditions as the slag pastes activated with OBFA and OBBA, although using an additional temperature: 25 °C. After the first 24 h all the specimens were removed from the moulds and stored in a humidity chamber at 21±2 ºC and 99 % RH for 2, 7 and 28 days.

Specimens (2, 7 and 28 days of curing) were tested for flexural strength on a Netzsch Geratebau testing machine and for compressive strength on an Autotest-200/10-SW test frame. Reactivity of the pastes was determined by conducting isothermal conduction calorimetry tests on the same geopolymer pastes prepared with the same liquid/solid ratios, used in mechanical strength studies, as the specimens (Table 1). The tests were run on a TAM Air isothermal conduction calorimeter for 180 h.

Table 1. Paste labels, mixes and curing conditions

Sample	SL (%wt)	CFA (% wt)	OBFA (% wt)	OBBA (% wt)	Temperature ºC	l/s	Liquid
SL-W 45	100	-	-	-	45	0.35	water
SL-W 85	100				85	0.35	water
SL-OBFA 70/30 45	70	-	30	-	45	0.35	water
SL-OBFA 70/30 85	70	-	30	-	85	0.35	water
SL-OBBA 70/30 45	70	-	-	30	45	0.32	water
SL-OBBA 70/30 85	70	-	-	30	85	0.32	water
CFA- OBFA 70/30 45	-	70	30	-	45	0.35	water
CFA- OBFA 70/30 85	-	70	30	-	85	0.35	water
CFA- OBBA 70/30 45	-	70	-	30	45	0.32	water
CFA- OBBA 70/30 45	-	70	-	30	85	0.32	water
SL-K 25	100	-	-	-	25	0.45	2.5 M KOH
SL-K- 45	100	-	-	-	45	0.45	2.5 M KOH
SL-K- 85	100	-	-	-	85	0.45	2.5 M KOH

2.3. Interaction of OBFA- and OBBA-activated pastes with the environment

In addition to evaluating the potential of OBFA and OBBA as alkaline activators, the interaction of the resulting geopolymer pastes with the environment had to be assessed to determine the viability of their actual use. The methodologies used in this part of the study are described in the following section.

2.3.1. Determination of radionuclide activity in alkali-activated pastes

The blends containing biomass ash and vitreous slag or coal fly ash were analysed for compliance with the European directive [51] on the use of NORM-bearing waste in construction materials by calculating their theoretical activity concentration indices. Those indices were determined as follows: i) calculation of the activity concentration of each isotope included in the index (*I*) in each blend; ii) calculation of the index for the blends by combining the indices for each material; and iii) calculation of the index for the resulting paste.

i. Concentration of each isotope in the mixes (Equation 3):

$$A_{Isotope_{Blend}} = A_{Isotope\_m1} \cdot P_{Blend\_m1} + A_{Isotope\_m2} \cdot P_{Blend\_m2} \quad (Eq.3)$$

where: $A_{Isotope\_Blend}$ is the activity concentration of the isotope in the blend; $A_{Isotope\_m1}$ the activity concentration of the isotope in material 1 in the blend; P_{Blend_m1} the percentage of material 1 in the blend; $A_{Isotope\_m2}$ the activity concentration of the isotope in material 2 in the blend; and P_{Blend_m2} the percentage of material 2 in the blend

The activity concentration uncertainties for the isotopes in the blends were calculated with Equation 4:

$$u(A_{Isotope_{Blend}}) = \sqrt{(P_{Blend\_m1})^2 \cdot u^2(A_{Isotope\_m1}) + (P_{Blend\_m2})^2 \cdot u^2(A_{Isotope\_m2})} \quad (Eq.4)$$

where: $u(A_{Isotope\_Blend})$ is the activity concentration uncertainty for the isotope in the blend; $u(A_{Isotope\_m1})$ the activity concentration uncertainty for the isotope in material 1 in the blend; and $u(A_{Isotope\_m2})$ the activity concentration uncertainty for the isotope in material 2 in the blend.

ii. Calculating the index in the blend by combining the indices in each material

Theoretical values for index *I* in the blends were determined from either the *I* values calculated with the aforementioned formulas or from Equation 5:

$$I_{Blend} = I_{m1} \cdot P_{Blend\_m1} + I_{m2} \cdot P_{Blend\_m2} \quad (Eq.5)$$

iii. Calculating the index in the pastes

The indices for the pastes were calculated from Equation 6:

$$I_{Hydrated\_Blend} = I_{Blend} \cdot P_{Hydrated\_Blend} \quad (Eq.6)$$

where: $I_{Hydrated\_Blend}$ is the index in the paste; and $P_{Hydrated\_Blend}$ the percentage of water in the blend.

The ^{210}Po and ^{210}Pb contents in the blends were also analysed as described in section 1 above.

These calculations drew from the values for the 28 d SL-W, SL-OBFA 70/30, SL-OBBA 70/30, CFA-OBBA 70/30 and CFA-OBFA 70/30 pastes.

2.3.2. Leaching study to test raw material and geopolymer paste interaction with the environment in the final stage of their life cycle

The OBFA and OBBA ash, vitreous slag (SL) and the two 28 d pastes, SL-OBFA-70/30 and SL-OBBA-70/30, cured at 45 °C and 85 °C were tested to an adapted version of the procedure for determining toxic substance leaching laid down in European standard EN 12457-2 [61]. The eluate collected was analysed to find its pH (on a Crison GLP 22 pH-meter) and electrical conductivity (on a Crison GLP 31 EC-meter). The elemental concentration in the resulting liquids was determined with the ICP-OES technique described in sub-section 2.2.1.

Gamma spectrometry proved to be insufficiently sensitive technique to determine the presence of radionuclides in the eluates from the pastes studied in this article. For that reason two elements, ^{210}Po and ^{210}Pb (members of the uranium series that can be determined with alpha spectrometry), were chosen on the grounds of their environmental significance and the low detection limit that it is reached with this instrumental technique. The quantification of both isotopes in the leached sampled were realised with the same procedure described in section 2.1 with little variations. A ^{208}Po tracer was added to a 100 ml aliquot of the liquid obtained from the metals lixiviation. The dissolution was evaporated until dryness at a low temperature <65ºC. After addition of chemical reagents to the solid, as it was indicated in the analytical procedure employed by Flynn, the polonium was auto-deposited on a silver disk. The ^{210}Pb was determined several months later, in the preserved supernatant of the first auto-deposited polonium, applying the same technique described previously. Due to the low detection limits reached for ^{210}Po and ^{210}Pb, these elements could be useful tools to quantify the lixiviation of natural radionuclides from complex materials and to predict their behaviour in the final stage of its life cycle.

3. RESULTS AND DISCUSSION

Main results obtained according to the three proposed objectives are discussed below.

3.1. Chemical, mineralogical, physical and radiological characterisation of slag and coal fly ash precursors and olive biomass ash

The chemical characterisation of all the materials is given in Table 2. The table also lists the loss on ignition, insoluble residue, reactive silica values for CFA, OBFA and OBBA and vitreous and glass content for SL and CFA, respectively. Particle size distribution of materials are shown in Table 3.

Table 2. Chemical composition (wt. %) of blast furnace slag (SL), coal fly ash (CFA), olive biomass fly ash (OBFA) and olive biomass bottom ash (OBBA)

Sample	SiO_2	Al_2O_3	Fe_2O_3	CaO	MgO	K_2O	Na_2O	P_2O_5	SO_3	TiO_2	V_2O_5	Cr_2O_3	MnO
SL	36.50	9.95	0.38	43.38	6.74	0.35		0.04		0.48	-	-	0.26
CFA	45.35	23.70	7.74	3.90	1.90	3.29		0.45		0.90	0.90	-	0.07
OBFA	12.60	2.97	2.30	20.21	4.85	26.34	1.12	3.84	4.00	0.24	-	0.02	0.06
OBBA	23.61	5.41	6.12	20.61	6.02	17.31	1.29	4.04	0.80	0.83	-	0.04	0.10

Sample	CuO	ZnO	SrO	ZrO_2	Rb_2O	Cl	LoI	IR	Reactive silica	Vitreous/glass content
SL	-	-	0.04	0.02	-	-	0	0.00	-	99
CFA	-	0.03	0.05	0.02	-	-	10.76	0.13	42.45	87.5
OBFA	0.10	0.02	0.08	0.02	0.01	2.82	18.40	-	11.10	-
OBBA	0.06	0.01	0.01	0.03	0.01	0.25	13.40	-	16.00	-

LoI: loss on Ignition IR: Insoluble Residue

Mineralogical characterisation of SL with XRD (Figure 1) revealed an amorphous hump with a 2θ maximum at 31º which confirm the high vitreous content of the slag. Crystalline phases as akermanite ($Ca_2Mg(Si_2O_7)$) and gehlenite ($Ca_2Al(AlSiO_7)$) were also found. The diffractogram for CFA contained also a hump at 2θ = 20º–35º and crystalline phases such as quartz (SiO_2), hematite (Fe_2O_3), magnetite ($Fe^{2+}Fe_2^{3+}O_4^{2-}$) and mullite ($Al_6Si_2O_{13}$) were also detected. XRD for OBBA presented a hump of moderate intensity with a 2θ maximum at 35º and a somewhat stronger signal in OBBA. The majority crystalline phases identified in the two types of ash were quartz (SiO_2), calcite ($CaCO_3$) and dolomite ($CaMg(CO_3)_2$). Similar mineralogies have been reported for olive biomass ash in the literature [62]. OBFA also contained aluminium oxalate ($C_6Al_2O_{12}$) and a magnesium potassium silicate ($K_2Mg(SiO_4)$). OBBA, in turn, contained minority phases such as kalsilite ($KAlSiO_4$), tremolite and an iron and sodium phosphate ($Na_{3.12}Fe_{2.44}(P_2O_7)_2$).

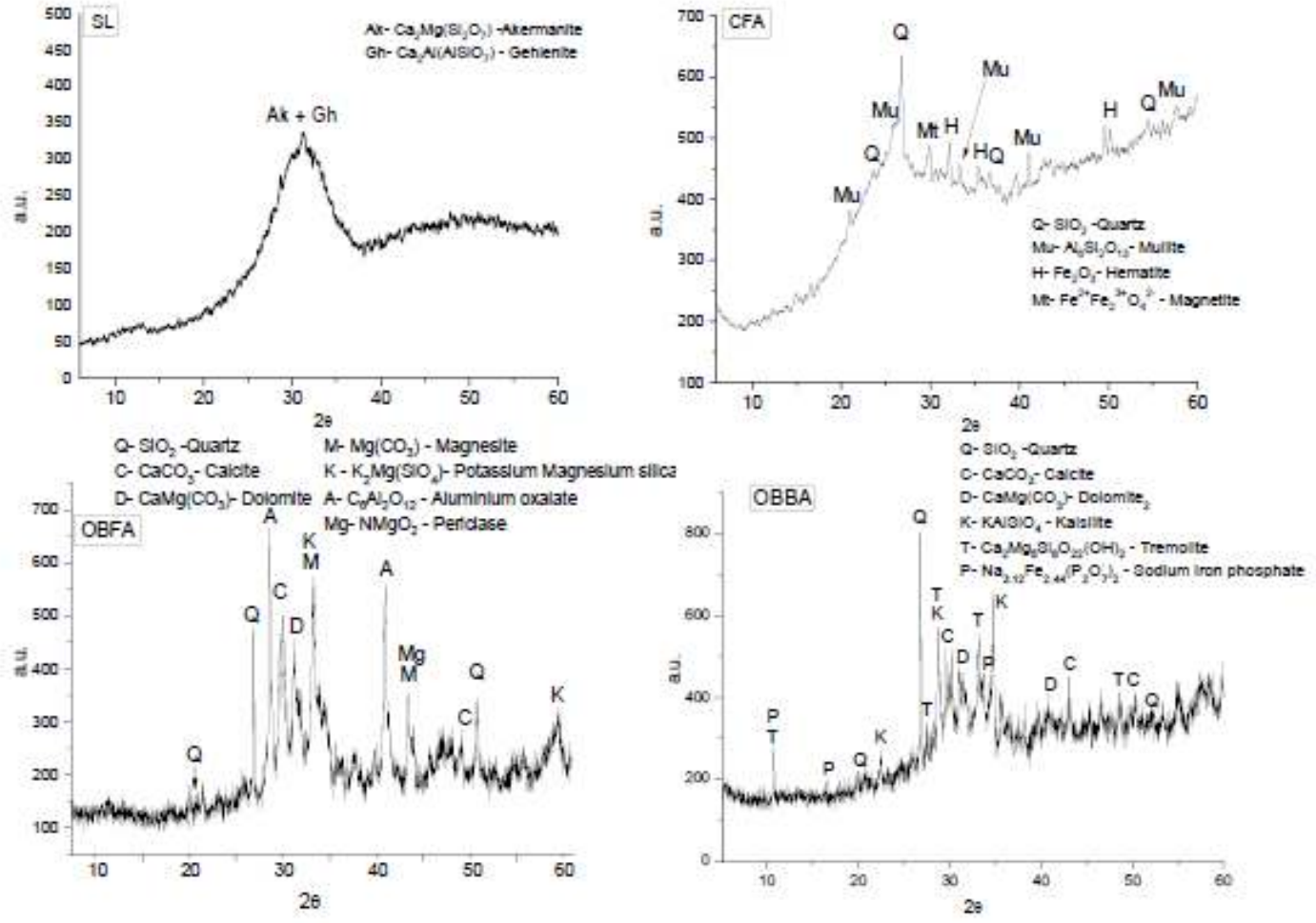

Figure 1. X-ray patterns for SL, CFA, OBFA and OBBA samples

Table 3. Particle size distribution and Blaine fineness for blast furnace slag (SL), coal fly ash (CFA), olive biomass fly ash (OBFA) and olive biomass bottom ash (OBBA)

Sample	d10: (10% of sample smaller than) (μm)	d50: (50% of sample smaller than) (μm)	d90: (90% of sample smaller than) (μm)	Blaine (m^2/kg)	Specific surface (m^2/g)*
SL	1.60	10.42	29.81	437	-
CFA	1.53	8.38	35.34	422	-
OBFA	1.56	11.89	39.61	-	1.54*
OBBA	1.34	10.09	40.01	-	1.73*

* Laser granulometric estimation

According to the methodology used for radiological characterization (see section 2.1), the radiological findings are given in Table 4.

Table 4. Activity concentration (in $Bq \cdot kg^{-1}$) and respective indices for the radionuclides in SL, CFA, OBFA and OBBA samples

Sample	^{238}U ($Bq \cdot Kg^{-1}$)					^{232}Th ($Bq \cdot Kg^{-1}$)				^{40}K ($Bq \cdot Kg^{-1}$)	Index
	^{234}Th	$^{214}Pb(^{226}Ra)$	^{214}Bi	^{210}Pb	^{210}Po	^{228}Ac	^{212}Bi	$^{212}Pb(^{232}Th)$	^{208}Tl		
SL	89.20 ±5.2	96.70±4.8	84.90±2.3	18.70±4.5	13.30±2.5	30 ±1.3	34 ±3.3	30.40 ±1.4	10.26 ±0.44	96.10 ±5.7	0.506±0.018
CFA	87.50 ±9.0	88.40±3.4	79.70±2.3	95±11	-	85.10 ±3	85.3 ±8.2	76.60 ±3	24.04 ±0.93	868±32	0.967±0.022
OBFA	< 10	11.87±0.8	10.85±0.64	88±13	85.50±7.4	7.10 ±1	< 12	6.30 ±0.43	2.32 ±025	5852±204	2.022±0.068
OBBA	< 3.7	9.10±0.85	9.53±0.61	14.50±6.1	8.30±2.4	6.50 ±1.3	7.1 ±4.3	5.96 ±0.55	1.75±0.10	35898±116	1.256±0.0039

* Shaded columns contain the data used to calculate the index. Uncertainties were calculated with a k factor of 2. The white background columns contain the data used to verify equilibrium in natural radioactive series. The value for thallium is 1/3 of the activity concentration of the other members of the decay chain.
The ^{210}Pb and ^{210}Po values were determined with alpha spectrometry.

Further to the data in Tables 2 and 3, the SL and CFA precursors had chemical, mineralogical and physical compositions characteristic of their nature, as referenced in earlier papers [63] [64] [65] [66] [67]. The chemical characterisation of OBFA and OBBA (Table 1) revealed a prevalence of K_2O, SiO_2 and CaO, along with smaller amounts of Al_2O_3 and high loss on ignition, as reported in the literature for olive biomass similar to the waste studied here [68] [37]. In the classification established in a study led by Vassilev [37], the biomass ash used here would lie in the general category for varieties of biomass used as a fuel, with olive waste included under sub-group 59 in the group '2.3 *Other waste (HAR, herbaceous and agricultural residue*)'. Also according to Vassilev et al. [37], the six primary oxides in that type of waste would be ranked, in terms of content, as follows:

$$K_2O > SiO_2 > CaO > P_2O_5 > MgO > Al_2O_3$$

which concurs very broadly with the content in the OBFA and OBBA used in this study. The explanation for the high K_2O content characteristic of this type of HAR ash is that due to intense yearly olive tree growth, its fruit contains high proportions of alkaline elements taken up directly from the soil [69]. At the same time, olive ash may be deduced to be scantly pozzolanic due to its low SiO_2 and reactive silica contents (Table 1) and scant proportion of Al_2O_3, further to reports by other authors [37] [41]. The reactive silica content in OBFA and OBBA and their chemical composition (Table 2), based primarily on CaO (≈20 wt. %), SiO_2 (12 wt. % to 23 wt. %) and K_2O (17 wt. % to 26 wt.%), suggest that they could be used as potentially activators in alkaline cement manufacture. Moreover, mineralogical findings were indicative of a need to study the potential of OBFA and OBBA as alkaline activators in greater depth.

As the data in Table 3 show, the objective of obtaining OBFA and OBBA samples with a size smaller than 45 μm has been reached and both ashes exhibited very similar particle size distribution.

With respect to the radiological results, these industrial raw materials (SL and CFA) had high natural uranium and thorium series radionuclide concentrations and a relatively low ^{40}K content (Table 4). ^{226}Ra activity concentrations were observed to be higher in SL and CFA than the mean 50 $Bq \cdot kg^{-1}$ for construction materials, whilst ^{232}Th activity concentration was lower than that mean value in SL and higher in CFA. The ^{40}K activity concentration in SL was lower than the mean 500 $Bq \cdot kg^{-1}$ estimated for construction materials and on the same order of magnitude in CFA. [70] [71]. ^{210}Po and ^{210}Pb present in SL (Table 4) lie in the same concentration range, which is an indication of radioactive equilibrium in this material (18.7±4.5 $Bq \cdot kg^{-1}$ (^{210}Pb) and 13.3±2.5 $Bq \cdot kg^{-1}$ (^{210}Po)). In CFA these two isotopes would be in radioactive equilibrium with the rest of the elements of the series (95±11 $Bq \cdot kg^{-1}$ (^{210}Pb) and 88.4±33.4 $Bq \cdot kg^{-1}$ (^{214}Pb)). The disequilibrium observed in the uranium series in SL (96.7±4.8 $Bq \cdot kg^{-1}$ for ^{214}Pb (^{226}Ra) and 18.7±4.5 $Bq \cdot kg^{-1}$ for ^{210}Pb) and not in the CFA (88.4±3.4 $Bq \cdot kg^{-1}$ for ^{214}Pb (^{226}Ra) and 95±11 $Bq \cdot kg^{-1}$ for ^{210}Pb) indicate the impact of furnace ignition temperature on the generation of these materials.

The biological origin of OBFA and OBBA determined the low activity concentrations of ^{226}Ra and ^{232}Th (Table 4), and high activity concentration of ^{40}K. The ^{210}Po + ^{210}Pb content was greater than theoretically expected in OBFA if the radionuclides belonging to the uranium series would have been in the material in secular radioactive equilibrium. In the biomass ashes the two isotopes (^{210}Po and ^{210}Pb) would have been in equilibrium because their concentrations showed similar values, considering the given measurement uncertainties: 88±13 $Bq \bullet kg^{-1}$ (^{210}Pb) and 85.5±7.4 $Bq \bullet kg^{-1}$ (^{210}Po) in OBFA; and 14.5±6.1 $Bq \bullet kg^{-1}$ (^{210}Pb) and 8.3±2.4 $Bq \bullet kg^{-1}$ (^{210}Po) in OBBA. The equilibrium observed in the uranium series in OBBA (9.1±0.85 $Bq \bullet kg^{-1}$ for ^{214}Pb (^{226}Ra) and 14.5±6.2 $Bq \bullet kg$-1 for 210Pb) and not in OBFA (11.87±0.80 $Bq \bullet kg^{-1}$ for ^{214}Pb (^{226}Ra) and 88±13 $Bq \bullet kg^{-1}$ for ^{210}Pb) again attested to the impact of furnace ignition temperature on the generation of both types of biomass ashes.

Olive oil industry waste has certain advantages and disadvantages relative to ash of mineral origin (coal). The advantages have to do with how natural series radionuclides are taken up into 'plant' biological material, in this case olive trees. Plants' ability to accumulate uranium varies widely. The soil-to-plant transfer factor (TF) (Bq per kg dry mass in plant tissue/ Bq per kg dry mass in soil) ranges across 6 orders of magnitude with a geometric mean of $2.27 \cdot 10^{-2}$ (geometric standard deviation, 9.1 $kg.kg^{-1}$) [72]. Olive tree (*Olea europeae*) TFs from soil to leaves and fruit are, for ^{40}K, 0.8 to 1.2; for ^{238}U, $2.8 \cdot 10^{-2}$ to $<5.0 \cdot 10^{-2}$; for ^{210}Po, 1.3 to $5.8 \cdot 10^{-2}$; and for ^{210}Pb, 1.2 to 0.2 [73]. As noted earlier, activity concentration was not found to be high for either uranium or thorium. Olive waste combustion temperature and its conversion to ash are suggestive of a low natural radionuclide content. The content in combustion ash can be inferred from the environmental concentration of uranium and thorium in the soil and their TFs. ^{40}K concentration in olive trees is very high (3000-10 000 $Bq \cdot kg^{-1}$], however, primarily due to the species' capacity to concentrate potassium. An olive tree producing 30 kg of olives leaches 560 g of K_2O. Potassium is the major nutrient for olive trees, higher even than nitrogen [74].

3.2. Viability of the use of OBFA and OBBA as potential geopolymer alkaline activators

As mentioned before, solubility of OBFA and OBFA in water was studied, as well as mechanical performance of pastes prepared with SL or CFA and olive biomass ashes. Main findings are discussed below.

3.2.1. OBFA and OBBA water solubility

The solubility findings and pH values at the three aforementioned temperatures (25º, 45º and 85º C) are listed in Table 5. The percentage of alkali (K and Na) solubilised relative to the starting content of each two elements is shaded in grey to highlight the high solubility of these alkaline elements.

Table 5. Elements solubilised (mM/L), percentage solubilised (in parenthesis- for S, Si, Al, Ca, Cr, Mg and P per cent extracted) and pH values in OBFA and OBBA at three test temperatures.

Sample	K	S	Na	Si	Al	Ca	Cr	Mg	P	pH
OBFA 25	255.58 (45.6)	37.97 (76)	15.24 (42.1)	4.21 (2.0)	0.59 (1.0)	0.32 (0.1)	0.02 (7.6)	0.002 (< 0.1)	0.05 (0.1)	12.92
OBFA 45	223.47 (39.9)	39.20 (78)	13.97 (38.7)	5.33 (2.5)	0.61 (1.0)	0.29 (0.1)	0.03 (11)	0.005 (< 0.1)	0.07 (0.1)	13.04
OBFA 85	276.34 (49.3)	33.71 (67)	20.13 (55.7)	8.59 (4.1)	0.55 (0.9)	0.31 (0.1)	0.03 (11)	0.100 (0.2)	0.15 (0.2)	13.26
OBBA 25	112.47 (30.5)	6.78 (68)	9,33 (22.4)	7.33 (1.9)	0.05 (0.05)	0.40 (0.1)	0.01 (1.9)	0.002 (< 0.1)	0.04 (0.1)	12.67
OBBA 45	109.50 (29.7)	6.75 (68)	9.62 (23.1)	8.35 (2.1)	0.07 (0.06)	0.31 (0.1)	0.01 (1.9)	0.001 (< 0.1)	0.06 (0.1)	12.77
OBBA 85	141.98 (38.5)	6.93 (69)	13.26 (31.8)	10.85 (2.8)	0.18 (0.2)	0.08 (0.02)	0.01 (1.9)	0.020 (< 0.1)	0.05 (0.1)	13.07

As a rule, higher test temperatures favoured ash solubility, with rising dissolved ion concentrations, for K in particular. More specifically, 45 % to 50 % of the K present in OBFA and 30 % to 38 % in OBBA was solubilised. Over 50 % of Na present in OBFA and 31 % in OBBA was also solubilised, although the starting quantities were much smaller (Table 1). Such a high K+Na content determined very basic pH values, suggesting that these two types of ash could potentially act as alkaline activators. Table 5 shows that in addition to K and Na, other elements were solubilised, S most intensely (67 % to 70 %) although due to its low content in OBFA and OBBA (Table 2) its solubilisation is not quite relevant, albeit subject to a heavy dependence on temperature, followed by Cr (1 % to 11 %) and Si (2 % to 4). Other elements were extracted in very low but measurable quantities. All these findings support the potential of theses ashes as an alternative alkaline activators, given its capacity to raise the alkaline content and pH in aqueous media to sufficiently high values.

3.2.2. Alkali-activated slag and coal fly ash pastes prepared with OBFA- and OBBA-as alkaline activators. Mechanical strengths and reactivity of the pastes

All the pastes were removed from the moulds after 24 h, but their behaviour varied depending on the blend and curing conditions. The SL-W pastes cured at 45 °C failed to harden, whereas those cured at 85 °C could be removed from the moulds and tested for mechanical strength. The SL-OBFA 70/30 and SL-OBBA 70/30 pastes hardened and could be tested. In contrast, as the CFA-OBFA 70/30 and CFA-OBBA 70/30 pastes also failed to harden after 24 h or even after 48 h, their mechanical performance could not be assessed. Two photographs of fly ash (CFA) and two of slag (SL) pastes are reproduced in Figure 2 by way of example. The still fresh CFA pastes exhibited rough edges and were slightly curved and broken. The condition of the 24 h slag pastes, in contrast, attested to their suitability for mechanical testing.

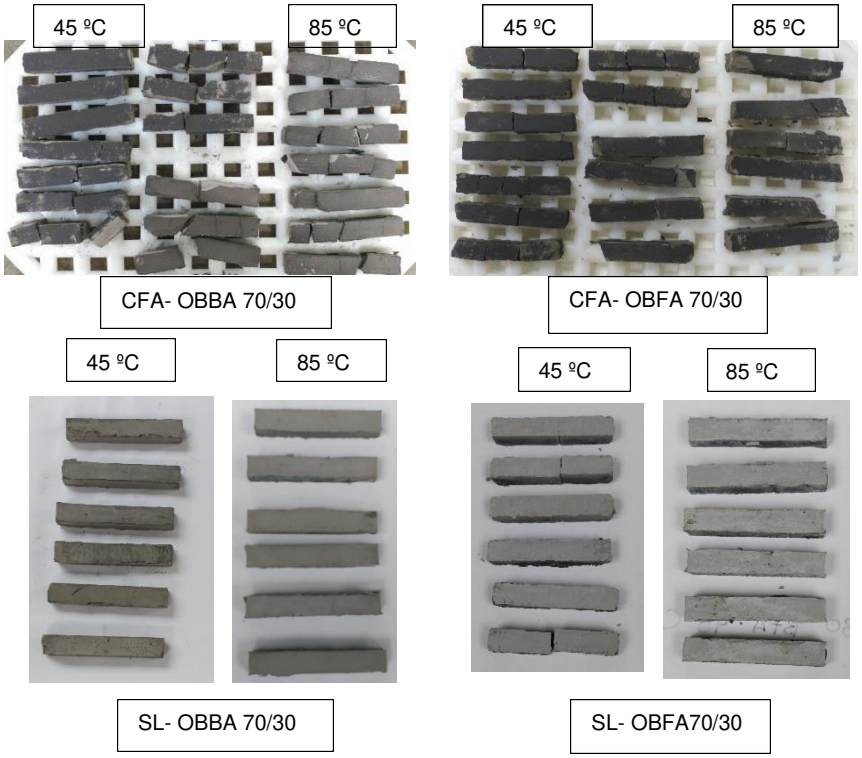

Figure 2. Alkali-activated CFA and SL pastes after curing

The anomalous behaviour observed in CFA-OBFA 70/30 and CFA-OBBA 70/30 pastes was attributable to the insufficiently high pH generated by the biomass ash (Table 5), for alkali-activated fly ash systems call for pH values of 13 to 14. [75].These findings differed from the results observed by Peys et al. [38], who activated pastes from other calcium-low aluminosilicates (metakaolin) with maize and oak/beech ash. Those authors attained pH values (13 to 14) higher than achieved in the present OBFA and OBBA solubility tests.

The flexural (Figure 3a) and compressive strength (Figure 3b) findings for the SL-W, SL-OBFA 70/30, SL-OBBA 70/30 and SL-K pastes at different curing temperatures are shown in Figure 3.

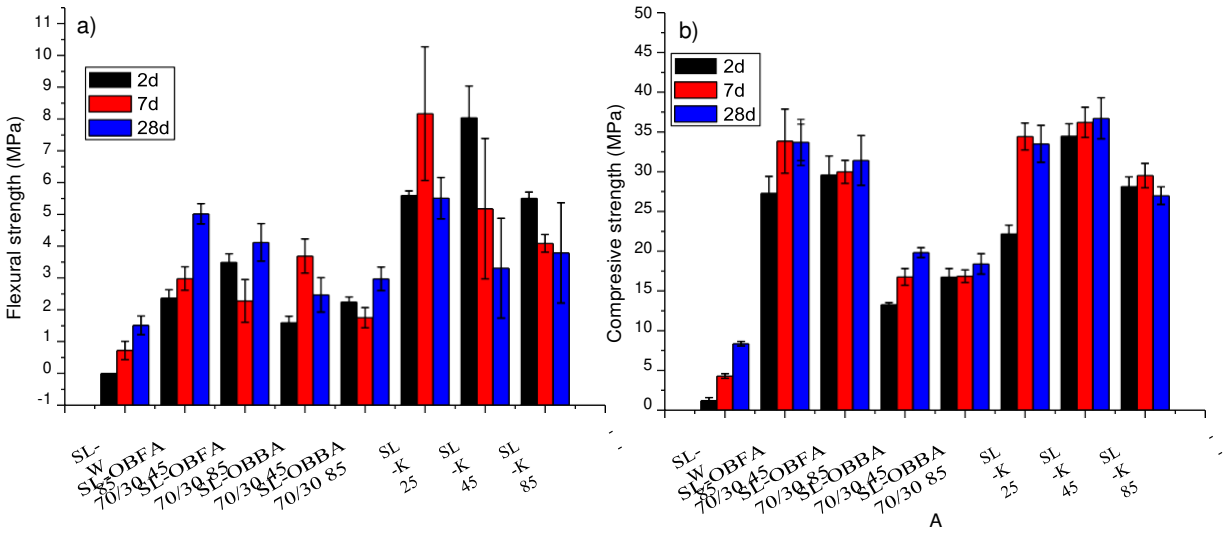

Figure 3. Flexural a) and compressive strength b) vs time in alkali-activated slag pastes

The alkali-activated slag pastes with OBFA or OBBA were observed to develop much greater flexural and compressive strength at all ages and curing temperatures than the SL pastes mixed with water only.

The 2 d SL-OBFA-70/30 mixes exhibited compressive strength values of 27 MPa to 30 MPa and the SL-OBBA-70/30 pastes of 13 MPa to 17 MPa, compared to just over 1 MPa in the SL-W 85 pastes. The inference is that the slag in these SL-OBFA-70/30 and SL-OBBA pastes was activated. Hydraulic reactions are known to take place very slowly in SL-W 85 materials [63] [76]. Curing temperature (45 °C vs 85 °C) showed no remarkable differences on strength in the SL-OBFA and SL-OBBA pastes, even though there were significant differences in the values of K and Na leached in the solubility test. Curing time (from 2 d to 28 d) appeared to have not very significant impact on strength. The SL-OBFA-70/30 pastes exhibited consistently higher (by around 40 %) flexural and compressive strength than the OBBA-activated materials.

An explanation for the mechanical behaviour described above was sought by conducting isothermal conduction calorimetry tests The findings are shown in Figure 4 and Table 6.

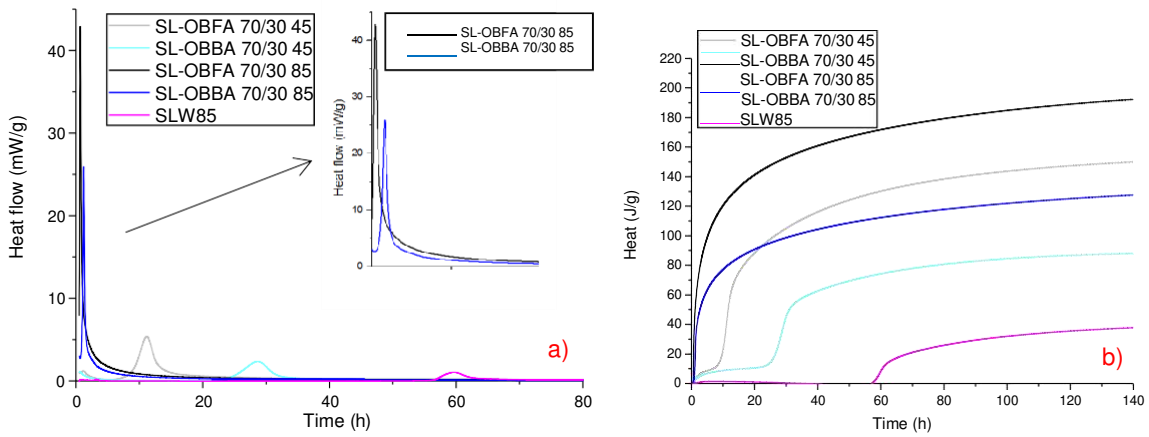

Figure 4. Isothermal conduction calorimetry results for pastes SLW 85, 70/30 SL-OBFA and 70/30 SL-OBBA at 45 °C and 85 °C: a) heat flow; b) total heat

Table 6. Calorimetric findings for activated slag pastes

Sample	Peak heat flow time (h)	Signal intensity (mW/g)	Total heat at 140 h (J/g)
SL-W 85	59.50	1.15	37
SL-OBFA 70/30 45	11.19	5.36	149
SL-OBFA 70/30 85	0.68	42.6	192
SL-OBBA 70/30 45	28.20	2.5	87
SL-OBBA 70/30 85	1.22	25.9	127

The SL-OBFA-70/30 pastes consistently exhibited more intense and earlier reactions than the SL-OBBA-70/30 pastes at both temperatures. The higher pH values and K and Na solubilisation percentages in the OBFA than the OBBA ash would explain the differences in reactivity and strength development in the two materials (Table 5). Earlier signal times were also observed with rising temperature in all the pastes, which would explain why 2 d strength was greater in the pastes activated at 85 °C than in the materials activated at 45 °C. In the SL-W 85 pastes, which exhibited the longest reaction times and lowest intensity, the lower mechanical strength could be attributed to the slower slag - water hydraulic reaction and therefore the delayed generation of reaction product (Figure 5) [63]. The reaction products in biomass ash-activated paste would be expected to be (N,K,C)-A-S-H-like gels [77]. Subsequent studies will be conducted to confirm that expectation.

The compressive strengths (Figure 3b) recorded at both temperatures for 28 d OBFA alkali-activated slag pastes were on the order of 30 MPa to 35 MPa, values comparable to those observed for KOH-activated slag. In contrast, the OBBA-activated pastes yielded 28 d mechanical strength around 40 % lower than pastes activated with KOH. One important factor to be borne in mind in this regard is that the SL-K paste contained 100 % slag, whereas the SL-OBFA and SL-OBBA pastes had 70 wt% slag and 30 wt% biomass ash. In addition, the pH in the OBFA (12.92 to 13.26) and OBBA (12.67 to 13.07) -activated samples was lower than in the KOH specimens (13.88), all of which indisputably affected strength development, even though the KOH-activated material required a higher liquid/solid ratio (Table 1).

The 28 d Strength Activity Index (SAI) for SL-OBFA-70/30 and SL-OBBA-70/30 given in Table 7 are the result of dividing the compressive strength of the OBFA- and OBBA-activated pastes at each temperature by the compressive strength observed in the respective KOH-activated systems. The data in Table 7 attest to a greater decline in strength than the 30 % slag replacement ratio only in the SL-OBFA-70/30-45. In SL-OBBA-70/30-45-bearing pastes and the SL-OBBA-70/30-85 pastes they decline in practically equal to that 30 % replacement. In the OBFA-activated pastes relative strength was around 1, affording proof that when dissolved in water, that biomass ash heightens the alkalinity in the medium, favouring the dissolution of and activating vitreous blast furnace slag. The aforementioned findings suggest that these ashes can potentially be used to alkali-activate blast furnace slag systems.

Table 7. 28 days compressive strength activity index for OBFA- and OBBA-activated slag pastes

Sample	SAI
SL-OBFA 70/30 45	0.92
SL-OBFA 70/30 85	1.16
SL-OBBA 70/30 45	0.54
SL-OBBA 70/30 85	0.68

3.3. Interaction of OBFA and OBBA activated pastes with the environment

The possibility that construction materials would leach naturally radioactive elements into the environment is of great importance. Thus leaching studies are essential to corroborate that the use of these new building materials does not involve risks to health or the environment.

3.3.1. Determination of radionuclide activity in alkali-activated slag pastes

The activity concentration findings for radionuclides in the geopolymers formed with slag/biomass ash and coal fly ash/biomass ash, the (*I*) index and the concentration of isotopes ^{210}Pb and ^{210}Po are given in Table 8. The radiological calculations for these pastes showed that OBFA- and OBBA-bearing pastes were apt for use in construction, as they conformed to European legislation on protection against exposure to ionising radiation, for the activity concentration index (ACI) found was less than 1 in all these materials. The methodology used was validated in earlier papers [78]. Different correction factors, suggested by Croymans et al. [79], may be applied to the index for the various conditions defined in the legislation, depending on the density and thickness of the end construction material. ^{210}Pb and ^{210}Pb were observed to be in disequilibrium with their parents in the decay chain due to the disequilibrium in the starting material.

Table 8: Radiological calculations of OBFA- and OBBA-bearing geopolymer pastes

Material Blends	^{238}U ($Bq \cdot kg^{-1}$)					^{232}Th ($Bq \cdot kg^{-1}$)				^{40}K ($Bq \cdot kg^{-1}$)	ACI raw or blend	ACI hydrated blend
	^{234}Th	$^{214}Pb(^{226}Ra)$	^{214}Bi	^{210}Pb	^{210}Po	^{228}Ac	^{212}Bi	$^{212}Pb(^{232}Th)$	^{208}Tl			
SL-W	66.1 ± 3.9	71.6 ± 3.6	62.9 ± 1.7	13.9 ± 3.3	9.9 ± 1.9	22.22 ± 0.96	25.2 ± 2.4	22.5 ± 1	7.6 ± 0.33	71.2 ± 4.2	---	0.375±0.013
SL-OBFA 70/30	65.4 ± 3.6	71.2 ± 3.4	62.7 ± 1.6	39.5 ± 3.9	35.0 ± 2.2	23.13 ± 0.96	23.8 ± 2.3	23.17 ± 0.99	7.88 ± 0.32	1823 ± 61	0.961±0.024	0.712±0.018
SL-OBBA 70/30	63.6 ± 3.6	70.4 ± 3.4	62.3 ± 1.6	17.4 ± 3.6	11.8 ± 1.9	22.95 ± 0.99	25.9 ± 2.6	23.07 ± 0.99	7.71 ± 0.31	1144 ± 35	0.731±0.017	0.554±0.013
CFA- OBFA 70/30	64.2 ± 6.3	65.4 ± 2.4	59.0 ± 1.6	92.9 ± 8.6	------*	61.7 ± 2.1	59.7 ± 5.7	55.5 ± 2.1	17.52 ± 0.66	2363 ± 65	1.283±0.025	0.951±0.019
CFA- OBBA 70/30	62.4 ± 6.3	64.6 ± 2.4	58.6 ± 1.6	70.9 ± 7.7	------*	61.5 ± 2.1	61.8 ± 5.9	55.4 ± 2.1	17.35 ± 0.65	1684 ± 41	1.054±0.019	0.798±0.014

Shaded columns are the data used for calculating index. Uncertainties have been calculated with a k=2 factor. The other columns are shown for checking equilibrium in natural radioactive series. Thallium value is 1/3 of the concentration activity of the others members of the radioactive chain.
Slag hydrated (S-W). Slag+ Olive-stone biomass fly ash (S-OBFA). Slag+ Olive-stone biomass bottom ash (S-OBBA). Fly ash + Olive-stone biomass fly ash (CFA-OBFA) . Fly ash + Olive-stone biomass bottom ash (CFA-OBBA).
* Blends activity concentrations empirically calculated based on percentage of radionuclide in the raw material both industrial origin and bio-mass (not hydrated)

The advantage of using olive biomass-ashes as additions in construction materials is that either they have no natural uranium or thorium series radionuclides or the activity concentration of those elements is very low. As the activity concentration of ^{226}Ra (progenitor isotope of ^{222}Rn) is consequently very low, the material can be expected to release very small amounts ^{222}Rn. Nonetheless, the ^{210}Pb content in this type of biomass was found to be higher than predicted by secular equilibrium, for it is not totally supported by ^{226}Ra, as observed by Sheppard et al. [80] in their study of disequilibrium in several Canadian plant species. Radon is the key radionuclide for understanding such disequilibrium because it is located in the uranium series between the ^{226}Ra and ^{210}Pb and, as a gas, very mobile. Although this isotope is produced in soils, some proportion nonetheless diffuses into the atmosphere, where its progeny is scavenged by dust particles and rain and deposited onto vegetation where it is absorbed through foliage. Plants thus obtain ^{210}Pb in foliage from three sources: a) direct uptake from soil, b) radioactive decay from ^{226}Ra or ^{222}Rn previously absorbed by the plant and c) foliar uptake of ^{210}Pb deposited on the leaves.

The drawback to using biomass ash is its very high ^{40}K content relative to other types of ash or mineral additions. The ^{40}K content can be measured directly with gamma spectrometry or inferred from the percentage of K_2O in the starting materials, which in some cases maybe over 50 wt. % (452 $g \cdot kg^{-1}$ of K is equivalent to 12 514 $Bq \cdot kg^{-1}$ of ^{40}K). The high external doses of radiation induced by ^{40}K gamma emissions constitute an obstacle to the use of olive biomass ash as a component of cementitious binders as it is contemplated in the index (Table 8), which however can be avoided, by controlling the amount of ash added.

3.3.2. Leaching study to test raw material and geopolymer paste interaction with the environment in the final stage of their life cycle

Raw material (SL, OBFA, OBBA) and activated slag paste (SL-OBFA-70/30 45, SL-OBFA-70/30- 85, 70/30 SL-OBBA-70/30- 45 and SL-OBBA-70/30-85) eluate conductivity, temperature and pH are given in Table 9, while Table 10 lists the metals that leached out of the slag (SL), biomass ash (OBBA and OBFA) and the pastes studied.

Table 9. Conductivity and pH determined in raw material and geopolymer paste eluates

	Conductivity		pH	
	Value mS/cm	°C	Value	°C
SL	0.34	21.0	12.49	22.0
OBFA	22.2	21.7	12.82	22.0
OBBA	11.38	21.5	12.59	22.0
SL-OBFA-70/30 45 pastes	8.39	22.2	12.45	22.0
SL-OBFA-70/30 85 pastes	5.18	22.5	12.51	22.0
SL-OBBA-70/30 45 pastes	3.51	22.4	12.01	22.0
SL-OBBA-70/30 85 pastes	2.74	21.9	12.22	22.0

A comparison of precursor (SL, OBFA and OBBA) and paste conductivity revealed lower salinity in the paste than in the raw material eluates (Table 9), a logical result given that forming a paste entails generating reaction products that bond tightly to the elements present in (N,K,C)-A-S-H-like gels [77].

Table 10. Metals leaching out of raw materials and geopolymer pastes in mg/L (wt. % from initial content)

	Al	Ca	Cr	Cu	Fe	K	Mg	Mn	Na	P	S	Si	Sr	Ti	Zn	Zr
SL	0.862 (0.016)	70.94 (0.23)	<0.008 (-)	<0.006 (-)	<0.01 (-)	3.915 (1.3)	0.336 (0.008)	<0.002 (<0.001)	4.816 (2.5)	<0.047 (<0.27)	15.37 (2.7)	21.24 (0.12)	0.092 (0.25)	<0.044 (<0.015)	<0.002 (-)	<0.025 (<0.17)
OBFA	13.414 (0.85)	20.3 (0.14)	1.625 (12.0)	0.015 (0.19)	<0.01 (-)	13978 (64.0)	<0.001 (-)	<0.002 (<0.004)	370.5 (45.0)	2.902 (0.17)	1405 (88.0)	144.8 (2.5)	0.074 (0.11)	<0.044 (<0.031)	<0.002 (0.012)	<0.025 (0.17)
OBBA	2.122 (0.074)	17.592 (0.12)	0.634 (2.3)	0.174 (0.36)	<0.01 (-)	6946 (48.0)	0.029 (-)	<0.002 (<0.003)	228.7 (24.0)	<0.047 (<0.003)	168.3 (53.0)	204.3 (1.9)	0.069 (0.82)	<0.044 (<0.09)	<0.002 (<0.025)	<0.025 (<0.11)
SL-OBFA-70/30 45	4.627 (0.15)	15.14 (0.078)	<0.008 (<0.26)	<0.006 (<0.34)	<0.01 (-)	2050 (41.0)	<0.001 (<3.63)	<0.002 (<0.002)	126.9 (44.5)	<0.047 (<0.012)	222.8 (34)	89.43 (0.88)	0.056 (0.165)	<0.044 (<0.024)	<0.002 (<0.056)	<0.025 (<0.23)
SL-OBFA-70/30 85	6.073 (0.20)	11.86 (0.061)	<0.008 (<0.26)	<0.006 (<0.34)	<0.01 (-)	1870 (37.5)	<0.001 (<3.63)	<0.002 (<0.002)	126.3 (44.5)	<0.047 (<0.012)	227.0 (34.5)	80.11 (0.79)	0.0345 (0.1)	<0.044 (<0.024)	<0.002 (<0.056)	<0.025 (<0.23)
SL-OBBA-70/30 45	1.630 (0.048)	21.78 (0.11)	<0.008 (<0.13)	<0.006 (<0.05)	<0.01 (-)	863.3 (25.5)	0.0245 (0.001)	<0.002 (<0.002)	78.61 (24.5)	<0.047 (<0.012)	143.2 (38.5)	83.52 (0.73)	0.062 (0.295)	<0.044 (<0.017)	<0.002 (<0.11)	<0.025 (<0.20)
SL-OBBA-70/30 85	5.14 (0.15)	12.421 (0.063)	<0.008 (<0.13)	<0.006 (<0.05)	<0.01 (-)	2231 (66.0)	<0.001 (<1.7)	<0.002 (<0.002)	119.1 (38)	<0.047 (<0.012)	250.9 (67)	92.81 (0.81)	0.032 (0.15)	<0.044 (<0.017)	<0.002 (<0.11)	<0.025 (<0.20)

Eluate conductivity was lower in the SL than in OBFA and OBBA samples, corroborating the lower Na and K content in the former (Table 1). Less of these cations leached out of SL (Table 10), with just 1.3 wt. % (K) and 2.5 wt. % (Na) compared to 24 wt. % (Na) and 48 wt. % (K) in OBFA and 45 wt. % (Na) and 64 wt. % (K) in OBBA. Conductivity was higher in OBFA than in OBBA (Table 9) due to the higher solubilised (Table 5) potassium content in the former. However, OBFA leaches lower amount of K than OBBA. Direct leaching of S from the raw materials was high, at 50 wt. % from OBFA and 80 wt. % from OBBA, while chromium followed a similar pattern: 2.3 wt. % from OBFA and 12 wt. % from OBBA. Given those values, in the event of direct deposition of the ash in the soil, OBBA would have a greater impact than OBFA. For elements with lower leaching percentages, such as Al (0.074 wt. % for OBFA

and 0.85 wt. % for OBBA) and Si (1.9 wt. % for OBFA and 2.5 wt. % for OBBA), the use of OBFA, would be preferred given the lower amount of aluminium leached. For elements such as Ca, Cu, Mg, P, Ti, Zr, Mn, Ve or Zn, with low leaching percentages (<0.5 wt. %), the implications of using one type of ash rather than the other would be negligible. Under such conditions direct deposition of the ash in the soil would have a greater or lesser impact depending on the element studied, which would have to be compared to the impact of the geopolymer (containing this ash) when stockpiled or otherwise disposed of at the end of its life cycle.

The differential leaching of elements from SL-OBFA-70/30 and SL-OBBA-70/30 pastes should also be borne in mind when choosing to use fly or bottom biomass ash, in light of the possible environmental impact involved. In pastes cured at 45 °C, elements Al, K, Na and Si leach more readily from SL-OBFA than SL-OBBA and Ca, S and Sr less readily from the former than the latter. In the materials cured at 85 °C, Al and Na were more leachable from SL-OBFA, whereas more K and Si leached out of SL-OBBA. Some elements, despite being constituents in the original material, such as Fe, Mn, P and Ti, barely leached at all, with percentages of under 0.024 wt. %. Others such as Zn, Zr, Cr and Cu leached at less than 0.34 wt. %. The amount recorded for Cr (<0.13 wt. % in SL-OBBA and <0.26 wt. % in SL-OBFA) was strikingly low compared to the 12 wt. % in the raw OBBA and 2 wt. % in the raw OBFA. Further to the aforementioned findings, the environmental impact of metals leaching directly out of the materials in the geopolymers at the end of their life cycle as construction materials would be lighter than the impact of depositing the ash directly in the soil.

Table 11. Comparison of obtained values (mg [element]/kg [original sample]) to UE- limits (mg/kg - essay 10 l/kg) in various type of emplacement

Possible Landfill	Cr (L/S = 10L/kg)	Cu (L/S = 10L/kg)	Zn (L/S = 10L/kg)
	mg/kg dry matter	mg/kg dry matter	mg/kg dry matter
Waste acceptable at landfills for inert waste	0.5	2	4
Granural non-hazardous waste accepted in the same cell as stable, not reactive hazardous waste	10	50	50
Granural waste acceptable at landfills for hazardous waste	70	100	200
SL	<0.08	<0.06	<0.02
OBFA	16.25	0.15	<0.02
OBBA	6.34	1.74	<0.02
SL-OBFA-70/30 (45º)	<0.08	<0.06	<0.02
SL-OBFA-70/30 (85º)	<0.08	<0.06	<0.02
SL-OBBA-70/30 (45º)	<0.08	<0.06	<0.02
SL-OBBA-70/30 (85º)	<0.08	<0.06	<0.02

The European Council (2002) [81] establishes the criteria and procedures for the acceptance of solid wastes in landfills following Annex II of Directive 1999/31 / EC. The limits for the leached elements after the deposit of wastes in the landfills depend on the type of waste and landfill. The determination of the element leached from the wastes is performed with two standards (EN 12457 / 1-4) with different proportion of liquid/solid and different particle sizes (L / S = 2 L/kg and L / S = 10 L/kg) and other for the percolation C_0.

The content of the leachate is expressed as mg $_{[element]\ \_leached}$/kg $_{[solid]\ \_\ used\ in\ leaching}$. The results obtained from leaching using the standard EN 12457/2 are observed in Table 11. The elements Cu, Zn and Cr are the only ones that would be subject to control in the deposit of both the original ashes and the material formed with them. Comparing the results with the permitted limits only the Cr would have restrictions on the type of conventional landfill when the olive ashes are deposited directly: OBFA Cr [16.25 mg/kg] and OBBA Cr [6.34 mg/kg] with a leaching limit of Cr with the procedure Cr [0.5 mg/kg]. Materials prepared with the blend of two industrial wastes (SL-OBFA and SL-OBBA) and their subsequent release in the environment would not have any type of restriction since the amount leached is less than the limit of sensitivity of this element [Cr] <0.08 mg/kg, approximately 10 times below in the most restrictive landfill type for its deposit. The new construction materials that contain wastes from other industries, can contribute to forming inert compounds with harmful elements to the environment, once their lifespan life has ended.

The ^{210}Pb and ^{210}Po radionuclide content in the eluates leached through the starting materials and resulting dry matter is given in Table 12 and the same information for the pastes in Table 13.

Table 12. ^{210}Pb and ^{210}Po leaching out of raw materials

	^{210}Pb Activity concentration (solid and liquid) ± 2s (k=2)			^{210}Po Activity concentration (solid and liquid) ± 2s (k=2)		
Raw material	Solid	Liquid	Percentage leached	Solid	Liquid	Percentage leached
	$Bq \cdot kg^{-1}$	$Bq \cdot L^{-1}$	%	$Bq \cdot kg^{-1}$	$Bq \cdot L^{-1}$	%
SL	18.7 ± 4.5	0.019 ± 0.012	1.04 ± 0.67	13.3 ± 2.5	0.0133 ± 0.0063	0.99 ± 0.51
OBFA	88 ± 13	< 0.021	< 0.24	85.5 ± 7.4	< 0.0096	< 0.11
OBBA	14.5 ± 6.1	< 0.024	< 1.7	8.3 ± 2.4	< 0.012	< 1.5

Table 13. ^{210}Pb and ^{210}Po leaching out of geopolymer pastes

		^{210}Pb Activity concentration (solid and liquid) ± 2s (k=2)			^{210}Po Activity concentration (solid and liquid) ± 2s (k=2)		
		Solid	Liquid	Percentage leached	Solid	Liquid	Percentage leached
		$Bq \cdot kg^{-1}$	$Bq \cdot L^{-1}$	%	$Bq \cdot kg^{-1}$	$Bq \cdot L^{-1}$	%
SL-OBFA 70/30 45 ºC	A	27.9 ± 6.1	< 0.021	< 0.77	31.4 ± 3.8	0.014 ± 0.0063	0.44 ± 0.21
SL-OBFA 70/30 45 ºC	B		< 0.0064	< 0.92		0.0097 ± 0.0051	0.31 ± 0.17
Average Value			---	---		0.0119 ± 0.0041	0.33 ± 0.14
SL-OBFA 70/30 85 ºC	A	27.5 ± 5.6	< 0.018	< 0.64	38.5 ± 4.4	<0.01	< 0.26
SL-OBFA 70/30 85 ºC	B		< 0.0069	< 1		0.0174 ± 0.0071	0.45 ± 0.19
Average Value			---	---		----	----
SL-OBBA 70/30 45 ºC	A	13.1 ± 3	< 0.02	< 1.6	13 ± 2.1	0.011 ± 0.0053	0.84 ± 0.43
SL-OBBA 70/30 45 ºC	B		< 0.0052	< 1.6		0.0112 ± 0.0059	0.86 ± 0.48
Average Value			---	---		0.0111 ± 0.004	0.85 ± 0.32
SL-OBBA 70/30 85 ºC	A	13.5 ± 3	< 0.018	< 1.4	13.9 ± 1.9	0.011 ± 0.0048	0.79 ± 0.36
SL-OBBA 70/30 85 ºC	B		< 0.0085	< 2.5		<0.13	<0.96
Average Value			---	---		---	----

The two key characteristics of biomass in connection with naturally occurring radioactive elements are that: a) due to their chemical properties, elements may be absorbed at different rates by plants, altering the equilibrium among the components of the decay chain; and b) air-borne natural elements may accumulate on leaves by direct deposition (^{222}Rn gas converts to ^{210}Pb that is adhered to aerosols and deposited or setlled on leaves) or indirect absorption in leaves via ingress of Rn through their stomas.

Once the radioactive equilibrium is altered, further disequilibrium may appear between parents and progeny, for biomass ash is generated at high temperatures [82]. Combustion may alter the transitory equilibrium between radionuclides by forming new compounds, inasmuch as some radionuclides, such as ^{210}Po, may be volatile. After disappearing from the ash, generally into the atmosphere, the ^{210}Po is re-generated by its parent ^{210}Pb (a scantly volatile element) to restore equilibrium. As ^{210}Po and ^{210}Pb are positioned after ^{222}Rn in the decay chain, they constitute useful tools for verifying the leach-out of elements located at the end of such chains.

The data on direct ^{210}Po and ^{210}Pb leaching from the raw materials showed that both elements leach more readily from slag than from OBFA or OBBA (Table 11). Slag deposited directly in the soil would leach 1 % of the initial quantity of ^{210}Pb and ^{210}Po, whereas the ash would leach from <0.24 % to 1.7 % of ^{210}Pb and <0.11 % to 1.5 % of ^{210}Po. Slightly less ^{210}Po was observed to leach from SL-OBFA-70/30-45 (0.33 %) than SL-OBBA-70/30-45 (0.85 %). The same trend was found at 85 °C (<0.26 % to 0.45 % for SL-OBFA-70/30-85 °C and 0.79 % to <0.96 % for 70/30 SL-OBBA-70/30-85 °C), but due to the uncertainty involved and the sensitivity limitations to the method, the values could not be verified. While no conclusions could be drawn for ^{210}Pb due to method sensitivity-related limitations, a similar trend might be expected. The leaching percentages of these elements were similar to the value found when Pb was added as a salt to geopolymer and hybrid pastes, as shown in earlier studies [78].

The presence of elements at the end of the decay chain in the eluates would not limit the use of biomass ash and slag blends. The presence of K might, however, for the high proportions in olive trees denote a high concentration of ^{40}K in both the pastes and the starting material. The 40 % to 52 % of ^{40}K calculated to leach is equivalent to an activity concentration in the eluate of 247 Bq·L^{-1} to 2067 Bq·L^{-1} in OBFA and 1217 Bq·L^{-1} to 1577 Bq·L^{-1} in OBBA, which would be discharged into the environment at the end of the life cycle.

4. Conclusions

From the chemical, mineralogical and radiology characterization of fly and bottom biomass ashes (OBFA and OBBA, respectively) generated during the combustion of olive oil industry waste, confirmed the high proportions of K_2O, SiO_2 and CaO and low proportions of Al_2O_3 in their composition. The majority crystalline phases identified in the two types of ash were quartz (SiO_2), calcite ($CaCO_3$) and dolomite ($CaMg(CO_3)_2$). OBFA also contained aluminium oxalate ($C_6Al_2O_{12}$) and a magnesium potassium silicate ($K_2Mg(SiO_4)$). OBBA, in turn, contained minority phases such as kalsilite ($KAlSiO_4$), tremolite and an iron and sodium phosphate ($Na_{3.12}Fe_{2.44}(P_2O_7)_2$). The radiological characterisation of OBFA and OBBA revealed low ^{226}Ra and ^{232}Th and very high (>2) ^{40}K activity concentrations. The ^{210}Po and ^{210}Pb content were observed to be greater than it would be if the uranium series in OBFA were in secular equilibrium, whereas OBBA exhibited radioactive equilibrium in the uranium series. Those findings attest to the importance of combustion furnace temperature in the production of the two types of ash.

Water solubility tests showed that OBFA and OBBA released alkaline ions K and Na into the medium, affording a high alkaline content and a sufficiently high pH (12.5-13.2) to act as potentially alternative alkaline activators in the alkali-activated materials or geopolymers formations. Increasing the test temperature favoured ash solubility. OBFA exhibited higher K solubility and consequently higher pH values than OBBA. Pastes made with 70 wt. % vitreous blast furnace slag (SL) and 30 wt. % of OBFA or OBBA cured at 45 °C or 85 °C, yielded alkali-activated materials or geopolymers with 28 days mechanical strength of 33 MPa to 18 MPa. SL-OBFA pastes developed higher strength than the SL-OBBA materials. In pastes prepared with 30 % wt. OBFA, strength values were comparable to those developed by slag pastes activated with a commercial KOH. However, the pastes made with 70 wt. % coal fly ash and 30 wt. % OBFA or OBBA proved to be inviable because the pH reached was not high enough to activate the precursor.

The radiological calculations for the geopolymer pastes prepared showed that OBFA- and OBBA-SL bearing pastes would conform to European legislation on protection against exposure to ionising radiation, for the activity concentration index (ACI) found in the final product was less than 1 in all cases. The pastes leached primarily K, a finding that should be analysed in detail in future research on the possible use of these materials. The presence of elements such as ^{210}Po and ^{210}Pb at the end of the decay chain in the eluates would not limit the use of biomass ash and slag blends. These findings have confirmed the feasibility of using olive oil industry biomass ashes as an alternative alkaline activator in blast furnace slag systems to produce alkali-activated materials or geopolymers, with properties that make them apt for use as building materials. In addition, they comply with the dose criteria laid down in European legislation, while minimising the environmental impact induced by the dispersal of toxic elements at the end of the service life of such materials.

Acknowledgements

Funding for the tests conducted in this study was provided by the Spanish Ministry of Economy, Industry and Competitiveness under projects BIA2013-47876-C2-1-P and BIA2016-77252-P. The authors thank A. Gil and P. Rivilla for their assistance in preparing the pastes and conducting the tests and E. González and L. García for performing the ^{210}Po and ^{210}Pb analyses in the different types of matrices of this study with the quality warrantied by its certification ENAC (Spanish National Accreditation Agency) in the determination of these elements in other environmental matrices

References

[1] International Development Association, "Special purpose financial statements and internal control reports of the International development association," 2005.

[2] Eurostat, "Europe in figures," 2012.

[3] J. Szulejko, P. Kumar, A. Deep and K. Kim, "Global warming projections to 2100 using simple CO2 greenhouse gas modelling and comments on CO2 climate sensitivity factor," *Atmospheric Pollution Research,* vol. 8, pp. 136-140, 2017.

[4] A. García-Maraver, M. Zamorano, A. Ramos-Ridao and L. Díaz, "Analysis of olive grove residual biomass potential for electric and thermal energy generation in Andalusia (Spain)," *Renewable and sustainable energy reviws,* vol. 16, pp. 745-751, 2012.

[5] I. Dincer, «Renewable energy and sustainable development: a crucial review.,» *Renewable and Sustainable Energy Reviews,* vol. 4, nº 2, pp. 157-175, 2000.

[6] S. Vassilev, D. Baxter, L. Andersen and C. Vassileva, "An overview of the composition and application of biomass ash. Part 1.Phase–mineral and chemical composition and classification," *Fuel,* vol. 105, pp. 40-76, 2013.

[7] F. Frandsen, «Utilizing biomass and waste for power production. A decade of contributing to the undestanding interpretation and analysis of deposits and corrosion products,» *Fuel,* vol. 84, nº 10, pp. 1277-1294, 2005.

[8] L. Wang, J. E. Hustad, Ø. Skreiberg, G. Skjevrak y M. Grønli, «A critical review on additives to reduce ash related operation problems in biomass combustion aplications,» *Energy Procedia,* vol. 20, pp. 20-29, 2012.

[9] J. Werther, M. Saenger, E. U. Hartge, T. Ogada y Z. Siagi, «Combustion of agricultural residues,» *Progress in energy and combustion science,* vol. 26, nº 1, pp. 1-27, 2000.

[10] P. McKendry, "Energy production from biomass (part 1): overview of biomass," *Bioresource Technology,* pp. 37-46, 2002.

[11] J. Kalembkiewicz and U. Chmielarz, "Ashes from co-combustion of coal and biomass: New industrial wastes," *Resources, Conservation and Recycling,* vol. 69, pp. 109-121, 2012.

[12] L. T.T. Vo and P. Navard, "Treatments of plant biomass for cementitious building materials – A review," *Construction and Building Materials,* vol. 121, pp. 161-176, 2016.

[13] A. Jaworek, T. Czech, T. Sobczyk and A. Krupa, "Properties of biomass vs. coal fly ashes deposited in electrostatic precipitator," *Journal of Electrostatics,* vol. 71, pp. 165-175, 2013.

[14] M. Camerani, B. Steenari, R. Sharma and R. Beckett, "Cd speciation in biomass ash particles after size separation by centrifugal SPLITT," *Fuel,* vol. 81, pp. 1739-1753, 2002.

[15] J. Sheperd, W. Buss, S. Sohi and K. Heal, "Bioavailability of P, other nutrients and potentially toxic elements from marginal biomass-derived biochar assessed in barley growth experiments," *Science of the Total Environment,* no. 584-585, pp. 448-457, 2017.

[16] R. Masto, E. Sarkar, J. George, K. Jyoti, P. Dutta and L. Ram, "PAHs and potentially toxic elements in the fly ash and bed ash of biomass fired power plants," *Fuel Processing Technology,* vol. 132, pp. 139-152, 2015.

[17] CEDEX, «Catálogo de residuos utilizables en construcción,» [En línea]. Available: http://www.cedexmateriales.es/catalogo-de-residuos/23/cenizas-procedentes-de-la-incineracion-de-biomasa/. [Último acceso: 10 2017].

[18] P. McKendry, «Energy production from biomass (part 1): overview of biomass,» *Bioresourc,* vol. 83, pp. 37-46, 2002.

[19] L. Nunes, J. Matias and J. Catalao, "Biomass in the generation of electricity in Portugal: A review," *Renewable and Sustainable Energy Reviews,* vol. 71, pp. 373-378, 2017.

[20] S. Vassilev, D. Baxter, L. Andersen and C. Vassileva, "An overview of the composition and application of biomass ash. Part 2. potential utilisation, technological and ecological advantages and challenges," *Fuel,* vol. 105, pp. 19-39, 2013.

[21] M. Freire, H. Lopes and L. Tarelho, "Critical aspects of biomass ashes utilization in soils: Composition,leachability, PAH and PCDD/F," *Waste Management,* vol. 46, p. 304.315, 2015.

[22] A. Demeyer, J. Voundi Nkana and M. Verloo, "Characteristics of wood ash and influence on soil properties and nutrient uptake: an overview," *Bioresources Technology,* vol. 77, pp. 287-295, 2001.

[23] M. Izquierdo and X. Querol, "Leaching behaviour of elements from coal combustion," *International Journal of Coal Geology,* vol. 94, pp. 54-66, 2012.

[24] N. Quaranta, M. Unsen, H. Lopez, C. Giansiracusa, J. Roether and A. Boccaccini, "Ash from sunflower husk as raw material for ceramic products," *Ceramics International,* pp. 147-153, 2011.

[25] V. Gupta, C. Jain, I. Ali, M. Sharma and V. Saini, "Removal of cadmium and nickel rom wastewater using bagasse fly ash – a sugar industry waste," *Water Research,* vol. 37, pp. 4038-4044, 2003.

[26] M. Zain, M. Islam, F. Mahmud and M. Jamil, "Production of rice husk ash for use in concrete as supplementary cementitious material," *Construction and building materials,* vol. 25, pp. 798-805, 2011.

[27] E. Villar-Cociña, E. Valencia Morales, S. Santo, H. Savastano and M. Frias, "Pozzolanic behaviour of bamboo leaf ash: characterization and determination of the kinetic parameters," *Cement and Concrete Composites,* vol. 33, pp. 68-73, 2011.

[28] E. Arif, M. Clark and N. Lake, "sugarcane bagasse ash from a high efficiency co-generation boiler: applications in cement and mortar production," *Construction and building materials,* vol. 128, pp. 287-297, 2016.

[29] R. González-Kunz, P. Pineda, A. Bras and L. Morillas, "Plant biomass ashes in cement-based building materials. Feasibility as eco-efficient structural mortars and grouts," *Sustainable cities and society,* vol. 31, pp. 151-172, 2017.

[30] J. Lessard, A. Omran, A. Tagnit-Hamou and R. Gagne, "Feasibility of using biomass fly and bottom ashes in dry-cast concrete production," *Construction and Building Materials,* vol. 132, pp. 565-577, 2017.

[31] M. Velay-Lizancos, M. Azenha, I. Martinez-Lage and P. Vázquez-Burgo, "Addition of biomass ash in concrete: Effects on E-Modulus, electrical conductivity at early ages and their correlation," *Construction and Building Materials,* vol. 157, pp. 1126-1132, 2017.

[32] R. Modolo, T. Silva, L. Senff, L. Tarelho, J. Labrincha, V. Ferreira and L. Silva, "Bottom ash from biomass combustion in BFB and its use in adhesive-mortars," *Fuel Processing Technology,* vol. 129, pp. 192-202, 2015.

[33] M. Villaquirán-Caicedo, R. Mejía de Gitierrez and N. Gallego, "A Novel MK-based geopolymer composite activated with rice husk ash and KOH: Performance at high temperature," *Materiales de Construcción,* vol. 67, no. 326, p. e117, 2017.

[34] C. Shearer, J. Provis, S. Bernal and K. Kurtis, "Alkali-activation potential of biomass-coal co-fired fly ash," *Cement and Concrete Composites,* vol. 73, pp. 62-74, 2016.

[35] J. Moraes, M. Tashima, J. Akasaki, J. Melges, J. Monzó, M. Borrachero, L. Soriano and J. Payá, "Effect of sugar cane straw ash (SCSA) as solid precursor and the alkaline activator composition on alkali-activated binders based on blast furnace slag," *Construction and Building Materials,* vol. 144, pp. 214-224, 2015.

[36] J. Payá, J. Monzó, M. Borrachero and M. Tashima, "Reuse of aluminosilicate industrial

waste materials in the production of alkali-activated concrete binders," in *Handbook of Alkali-Activated Cements, Mortars and Concretes*, Elsevier, 2015, pp. 487-518.

[37] S. Vassilev, D. Baxter, L. Andersen and C. Vassileva, "An overview of the chemical composition of biomass," *Fuel,* vol. 89, pp. 913-933, 2010.

[38] A. Peys, H. Rahier and Y. Pontikes, "Potassium-rich biomass ashes as activators in metakaolin-based inorganic polymers," *Applied Clay Science,* vol. 119, pp. 401-409, 2016.

[39] A. Font, L. Soriano, J. Moraes, M. Tashima, M. Borrachero and J. Payá, "A 100% waste-based alkali-activated material by using olive-stone biomass ash (OBA) and blast furnace slag (BFS)," *Materials Letters,* vol. 203, pp. 46-49, 2017.

[40] J. Barjol, "L'économie mondiale de l'huile d'olive," *Oilseeds, fats and lipids,* vol. 21, no. 5, 2014.

[41] J. Cuenca, J. Rodríguez, M. Martín-Morales, Z. Sánchez-Roldán and M. Zamorano, "Effects of olive residue biomass fly ash as filler in self-compacting concrete," *Construction and Building Materials,* vol. 40, pp. 702-709, 2013.

[42] M. Cruz-Yusta, I. Mármol, J. Morales and L. Sánchez, "Use of Olive Biomass Fly Ash in the Preparation of Environmentally friendly mortars," *Environmental science and technology,* vol. 45, pp. 6991-6996, 2011.

[43] D. Eliche-Quesada and J. Leite-Costa, " Use of bottom ash from olive pomace combustion in the production of eco-friendly fired clay bricks," *Waste Management,* vol. 40, pp. 323-333, 2016.

[44] D. Eliche-Quesada, M. Felipe-Sesé, A. Moreno-Molina, F. Franco and A. Infantes-Molina, " Investigation of using bottom or fly pine-olive pruning ash to produce environmental friendly ceramic materials," *Applied Clay Science,* vol. 135, pp. 333-346, 2017.

[45] J. de la Casa and E. Castro, "Recycling of washed olive pomace ash for fired clay brick manufacturing," *Construction and Building Materials,* vol. 61, pp. 320-326, 2014.

[46] M. Beltrán, A. Barbudo, F. Agrela, J. Jiménez and J. de Brito, " Mechanical performance of bedding mortars made with olive biomass bottom ash," *Construction and Building Materials,* vol. 112, pp. 699-707, 2016.

[47] J. Cuenca, J. Rodríguez, M. Martín-Morales, Z. Sánchez-Roldan and M. Zamorano, " Effects of olive residue biomass fly ash as filler in self-compacting concrete," *Construction and Building Materials,* vol. 40, pp. 702-709, 2013.

[48] J. Rosales, M. Cabrera, M. Beltrán, M. López and F. Agrela, "Effects of treatments on biomass bottom ash applied to the manufacture of cement mortars," *Journal of Cleaner Production,* vol. 154, pp. 424-435, 2017.

[49] J. e. a. Labrincha, "From NORM by products to building materials," in *Naturally ocurring radioactive materials in construction*, Elsevier, 2017.

[50] M. Martín-Morales, M. Alonso, S. Gismera, C. Gascó, M. Zamorano and F. Puertas, "Biomass ashes characterization and radiological behavior," in *Final Symposium NORM4Building Cost Action*, Rome, 2017.

[51] EU Council Directive 2013/59/Euratom, *basic safety standards for protection against the dangers arising from exposure to ionising radiation and repealing Directives 89/618/Euratom, 90/641/Euratom, 96/29/Euratom, 97/43/Euratom and 2003/122/Euratom.,* 2014.

[52] *UNE-EN 196-2 "Method of testing cement- Part 2: Chemical analysis",* 2014.

[53] *UNE 80230 "Methods of testing cement. Chemical analysis. Alternative methods",* 2010.

[54] U. 80-225-93, *Métodos de ensayo de cementos. Análisis químico. Determinación del óxido de silicio (SiO2) reactivo en los cementos, en las puzolanas y en las cenizas volantes,* 1993.

[55] R. Hooton and J. Emery, "Glass content determination and strength development predictions for vitrified blast furnace slag," in *First Int. Conf. on the fly ash, silica fume, slag and other mineral by products in concrete*, Montebello, Quebec, Canada,, 1983.

[56] P. Arjuman, M. Silbee and D. Roy, "Quantitative determination of the crystalline and amorphous phases in," in *10th International Congress on the Chemistry of Cement*, Gotheburg, Sweden, 1997.

[57] *UNE 80122. Methods of testing cement. Determination of fineness,* 1991.

[58] F. Puertas, M. Alonso, M. Torres-Carrasco, P. Rivilla, C. Gasco, L. Yagüe, J. Suárez y N. Navarro, «Radiological characterization of anhydrous/hydrated cements and geopolymers,» *Construction and Building Materials,* vol. 101, pp. 1105-1112, 2015.

[59] W.W.Flynn, «The determination of low levels of polonium-210 in environmental materials,» *Anal. Chim. Acta,* vol. 43, pp. 221-227, 1968.

[60] H. Bateman, «Solution of a system of differential equations occurring in the theory of radioactive transformations,» *Proc. Cambridge. Philos. Soc.,* vol. 15, pp. 423-427, 1910.

[61] U.-E. 12457-2, *Characterization of waste. Leaching. Compliance test for leaching of granular waste materials and sludges. Part 1 One stage batch test at a liquid to solid ratio of 10 l/kg for materials with high solid content and with particle size below 4 mm (without o,* 2003.

[62] P. Ochecova, P. Tlustos and J. Szakova, "Wheat and Soil Response to Wood Fly Ash Application in Contaminated Soils," *Agronomy Journal,* vol. 106, no. 3, pp. 995-1002, 2014.

[63] F. Puertas, «Escorias de alto horno: composición y comportamiento hidráulico,» *Mater. Construcc.,* vol. 43, nº 229, pp. 37-48, 1993.

[64] M. Palacios, M. Alonso, C. Varga y F. Puertas, «Influence of the alkaline solution and temperature on the rheology and reactivity of alkali-activated fly ash pastes,» *Cement and Concrete Composites,* accepted 2018.

[65] A. Fernández-Jimenez y A. Palomo, «Composition and microstructure of alkali activated fly ash binder: Effect of the activator,» *Cement and Concrete Research,* vol. 35, pp. 1984-1992, 2005.

[66] A. Hoyos-Montilla, Y. Arias-Jaramillo y J. Tobón, «Evaluation of cements obtained by alkali-activated coal ash with NaOH cured at low temperatures,» *Mater. Construcc.,* vol. 68, nº 332, 2018.

[67] S. Bernal, R. Mejía de Gutiérrez, E. Rodríguez, S. Delvasto y F. Puertas, «Mechanical behaviour of steel fibre-reinforced alkali activated slag concrete,» *Mater. Construcc.,* vol. 59, nº 293, 2009.

[68] A. Tortosa Masia, B. Buhre, R. Gupta and T. Wall, "Characterising ash of biomass and waste," *Fuel Processing Technology ,* vol. 88, pp. 1071-1081, 2007.

[69] T. Miles, J. Miles, L. Baxter, R. Bryers, B. Jenkins and L. Oden, "Boiler deposits from firing biomass fuels.," *Biomass Bioenergy,* vol. 10, pp. 125-138, 1996.

[70] T. Kovacs, G. Bator, W. Schroeyers, J. Labrincha, F. Puertas, M. Hegedus, D. Nicolaides, M. Sanjuan, P. Krivenko, I. Grubesa, Z. Sas, B. Michalik, M. Anagnostakis, I. Barisic, C. Nuccetell, R. Trevisi, T. Croymans, S. Schreurs y e. al, «From raw materials to NORM by products,» de *Naturally Occurring Radioactive Materials*, W. Schroeyers, Ed., Woodhead Publishing Series in Civil and Structural Engineering, 2017, pp. 135-182.

[71] R. Trevisi, S. Risica, M. DÁlessandro, D. Paradiso y C. Nuccetelli, «Natural radioactivity in building materials in the European Union: A database and an estimate of radiological significance,» *J. Environ. Radioact.,* vol. 105, pp. 11-20, 2012.

[72] D. Atwood, Radionuclides in the environment, J. W. $. sons, Ed., 2010.

[73] M. M.S. Al-Masri, B. Al-Akel, A. Nashawani, Y. Amin, K. Khalifa y F. Al-Ain, «Transfer of 40K, 238U, 210Pb, and 210Po from soil to plant in various locations in south of Syria,» *Journal of Environmental Radioactivity,,* vol. 99, nº 2, pp. 322-331, 2008.

[74] «Resumen del uso de potasio en el olivar,» [En línea]. Available: https://es.scribd.com/doc/130629727/Resumen-Del-Uso-de-Potasio-en-El-Olivar. [Último acceso: dec 2017].

[75] A. Fernández-Jímnez, A. Palomo y M. Criado, «Alkali activated fly ash binders. A

comparative study between sodium and potassium activators,» *Mater. Construcc.,* vol. 56, nº 281, pp. 51-65, 2006.

[76] R. Siddique and R. Bennacer, "Use of iron and steel industry by-product (GGBS) in cement paste and mortar," *Resources, Conservation and Recycling,* vol. 69, pp. 29-34, 2012.

[77] I. Garcia-Lodeiro, A. Palomo, A. Fernández-Jiménez y D. MacPhee, «Compatibility studies between N-A-S-H and C-A-S-H gels. Study in the ternary diagram Na2 O-CaO-Al2 O3 -SiO 2 -H2 O,» *Cement and Concrete Research,* vol. 41, nº 9, pp. 923-931, 2011.

[78] M. Alonso, A. Pasko, C. Gascó, J. Suarez, O. Kovalchuk, P. Krivenko y F. Puertas, «Radioactivity and Pb and Ni immobilization in SCM-bearing alkali-activated matrices,» *Construction and Building Materials,* vol. 159, pp. 745-754, 2018.

[79] T. Croymans, F. Leonardi, R. Trevisi, C. Nuccetelli, S. Schreurs y W. Schroeyers, «Gamma exposure from building materials – A dose model with expanded gamma lines from naturally occurring radionuclides applicable in non-standard,» *Construction and building materials,* vol. 159, pp. 768-778, 2018.

[80] S. Sheppard, M. Sheppard, M. Llin, J. Tait y B. Sanipelli, «Primordial radionuclides in Canadian background sites: secular equilibrium and isotopic differences,» *J. Environmental Radioactivity,* vol. 99, nº 6, pp. 933-946, 2008.

[81] E. Council, *Establishing criteria and procedures for the acceptance of waste at landfills pursuant to Article 16,* Official Journal of the European Communities, 2002.

[82] J. Mora, B. Robles, J. Corbacho, C. Gascó y M. Gázquez, «Modelling the behaviour of 210Po in high temperature processes,» *J. Environ. Radiact.,* vol. 102, nº 5, 2011.

[83] J. Ericksen, M. Gustin, D. Schorran, D. Johnson, S. Lindberg and J. Coleman, "Accumulation of atmospheric mercury in forest foliage," *Atmospheric Environment ,* vol. 37, pp. 1613-1622, 2003.

[84] R. Barbosa, N. Lapa, D. Dias and B. Mendes, "Concretes containing biomass ashes: Mechanical, chemical, and ecotoxic performances," *Construction and Building Materials,* vol. 48, pp. 457-463, 2013.

[85] G. sua-Iam and N. Makul, "Utilization of coal- and biomass-fired ash in the production of self consolidating concrete: a literature review," *Journal of Cleaner Production,* vol. 100, pp. 59-76, 2015.

[86] S. Bernal, E. Rodriguez, R. Mejía de Gutierrez and J. Provis, "Performance at high temperature of alkali-activated slag pastes produced with silica fume and rice husk ash based activators," *Materiales de Construcción,* vol. 65, no. 318, p. e049, 2015.

[87] V. Katare and M. Madurwar, "Experimental characterization of sugarcane biomass ash – A review," *Construction and Building Materials,* vol. 152, pp. 1-15, 2017